Defence Science Journal, Vol. 62, No. 6, November 2012, pp. 390-398, DOI: 10.14429/dsj.62.1428

Preparation and Characterisation of ε-CL-20 by Solvent Evaporation and Precipitation Methods

M. Ghosh, V. Venkatesan*, A.K. Sikder, and N. Sikder

High Energy Materials Research Laboratory, Pune-411 021, India
**E-mail: vvigcar@yahoo.com*

ABSTRACT

ε-CL-20 is prepared from raw CL-20 by solvent evaporation and precipitation methods. Experiments were also done using solvent evaporation coupled with in-situ ultrasonication method. Using precipitation method, ε-CL-20 is scaled up to 500 g batch. Raw CL-20 was assigned to α-CL-20. The chemical and polymorphic purity of prepared ε-CL-20 was found to be about 98 per cent and > 95 per cent, respectively. ε-CL-20 was obtained agglomeration free with well defined geometry in comparison with raw CL-20 and its crystal morphology is dominantly bi-pyramidal or lozenge crystal shapes. The obtained mean particle size of prepared ε-CL-20 by solvent evaporation method with and without in-situ ultrasonication and also by precipitation methods is about 30 µm - 40 µm, 150 µm - 200 µm and 150 µm - 300 µm, respectively. The measured true density of prepared ε-CL-20 by precipitation method with 100 g and 500 g batch scale using Helium gas pycnometer was 2.038 g/cm^3 and 2.043 g/cm^3, respectively. The lower value of calculated void percentage of ε-CL-20 (0.05-0.29%) indicate better crystal quality. Conclusively, prepared ε-CL20 has high true density with less percentage of voids, less total moisture content and free from agglomeration as compared with the starting raw CL-20 material.

Keywords: ε-CL-20, solvent evaporation, precipitation, ultrasonication, true density

1. INTRODUCTION

2,4,6,8,10,12-Hexanitro-2,4,6,8,10,12-hexaazaisowurtzitane (CL-20) is one of the most potential candidate for explosive and propellant formulations, which exhibits higher oxygen balance, density and heat of formation than the conventional energetic nitramines such as RDX and HMX. It was first synthesized by Nielson[1], *et al.* and later its explosive performance was found to be approximately 14 % higher than that of HMX[2]. Due to the presence of different molecular conformations and arrangements in lattice, CL-20 has been reported to exist in five different polymorphic forms. Four polymorphs (ε, β, α, and γ) exist at ambient condition and one (ζ) exists at high pressure[3-5]. Due to the high energetic performance, high density, and low sensitivity compared to the other polymorphs, ε-CL-20 is more desirable for use in propellant and weapons systems[2,3]. Hence, the preparation of ε-CL-20 with good crystal quality, desired particle size and crystal habit has been a great deal of interest in the view of high explosive and solid rocket propellant based formulations. Further, these physical characteristics of CL-20 play vital role in the sensitivity of CL-20[6]. Though worldwide researchers have been reported a few crystallisation methods[7,8] for the preparation of ε-CL-20, it is essential to optimize suitable crystallisation process to prepare as well to improve the quality of CL-20. The preparation of the desirable polymorph is possible by 'solvent – nonsolvent' technique which greatly help to improve crystal quality as well[9]. According to Foltz[5], *et al.*, it was shown that the β-form of crystals could be transformed to γ-one and then finally to ε-one by adjusting solvent and temperature for re-crystallisation. Correspondingly, the crystal density is also shifted from 1.98 g/cm^3 (β-form) to 2.044 g/cm^3 (ε-form) as with the structural transformation. Hoffman[10] reported the influence of the synthetic method of CL-20 on the crystal density of CL-20. Using nuclear quadruple resonance spectroscopic technique, Caulder[11], *et al*. studied the crystal quality of ε-CL-20 obtained from different precursors and solvent systems.

In the present study, it is focused to prepare and characterisation by both solvent evaporation and precipitation methods. The present evaporation method also relates for obtaining agglomeration free fine ε-CL-20 crystals by in-situ use of ultrasound to crystallisation solution. The obtained crystals were characterised using HPLC, FTIR, Raman, Powder XRD, SEM and DSC techniques. Particle size measurement of obtained ε-CL-20 was carried out using particle size analyser and true density by Helium gas pycnometer.

2. EXPERIMENTAL WORK

Raw CL-20 sample was obtained from Premier Explosive's Laboratories, India. All the solvents and allied chemicals used for the processes are of analytical grade with > 99 % purity. ε-CL-20 is prepared using both solvent evaporation and precipitation techniques. Raw CL-20 is dissolved in ethyl acetate solvent and then antisolvent, n-heptane is added into the solution to induce the crystallisation. For the effective recovery in the drowning-out crystallisation, the fraction of raw CL-20, ethyl acetate and n-heptane was applied as about from 1 : 15 : 35,

Received 12 January 2012, revised 23 October 2012, online published 12 November 2012

respectively in evaporation method, whereas 1 : 2 : 5 ratio was used in precipitation method. Then, free flowing white shiny crystals of ε-CL-20 were filtered, washed with n-heptane and dried. The crystallisation was also repeated using ultrasound of 35 kHz frequency with ultrasonic intensity level 80 % to study the effects of ε-CL-20 particle size and its crystal morphology. The solvent evaporation rate was controlled approximately from 2 ml/min to 4 ml/min in solvent evaporation method. In precipitation method, the stirring speed of CL-20 solution was kept about 150 rpm – 250 rpm and antisolvent, n-heptane addition rate was in the range of 40 ml/min – 50 ml/min. The mean particle size of prepared ε-CL-20 is largely dependent on solvent evaporation rate or antisolvent addition rate. Using both solvent evaporation and precipitation method, and several batches were conducted to establish the reproducibility of the method for preparation of ε-CL-20. ε-CL-20 was finally scaled up to 500 g batch level using precipitation method.

The prepared ε-CL-20 was well characterised using HPLC, vibrational spectroscopic, X-ray powder diffraction and scanning electron microscopic techniques. The IR spectrum (4000 - 400 cm^{-1}) of the ε-CL-20 was recorded using a Thermo Nicolet, USA, make Nicolet 5700 FTIR spectrometer with spectral resolution of 4 cm^{-1} and typically 64 scans were coadded to obtain good signal-to-noise ratio. The Raman spectrum (4000 – 100 cm^{-1}) of the ε-CL-20 was recorded using an In via Reflex dispersive Raman spectrometer from Renishaw, UK, with 2 scans at 2 cm^{-1} spectral resolution and at 0.1 % power filter of 300 mW laser power (Nd YAG 785 nm laser). Powder X-ray diffraction pattern of the ε-CL-20 was recorded using a PW3040/60 X'Pert PRO X-ray diffractometer from PAN analytical, Netherlands. Morphological information of the ε-CL-20 polymorphs ware obtained with a Quanta 200 Scanning Electron Microscope (SEM) from FEI, Netherlands. All the micrographs were recorded in low vacuum mode using a Large-Field Detector (LFD). The accelerating voltage was maintained within minimum required for image development and to prevent any charging up of samples and subsequent damages the particle surface. Particle size analysis of samples was carried out using the Hydro-2000MU particle size analyser from Malvern Instruments, UK. The analyser is based on the principle of laser light scattering with working range of particle size from 0.2 μ to 2000 μ. The true density of prepared ε-CL-20 and raw CL-20 has been measured by Quantachrome Helium gas ultrapycnometer 1000.

3. RESULTS AND DISCUSSION

Table 1 lists the recovery, chemical and polymorphic purity of prepared ε-CL-20 using solvent evaporation without and with in-situ ultrasonication and precipitation methods. In most of the batches, the sample recovery of prepared ε-CL-20 is about 85-90%. HPLC analysis showed the chemical purity of the prepared ε-CL-20 was about 98 %. Raw CL-20 used for the preparation of ε-CL-20 show higher degree of agglomeration with mean particle size of 185 μm Fig.1(a). The agglomerates consist of irregular crystal geometry, dominated by sharp edged diamond shape crystals. However, reprocessing of raw CL-20 in laboratory by solvent evaporation and precipitation methods show agglomeration free well defined crystals

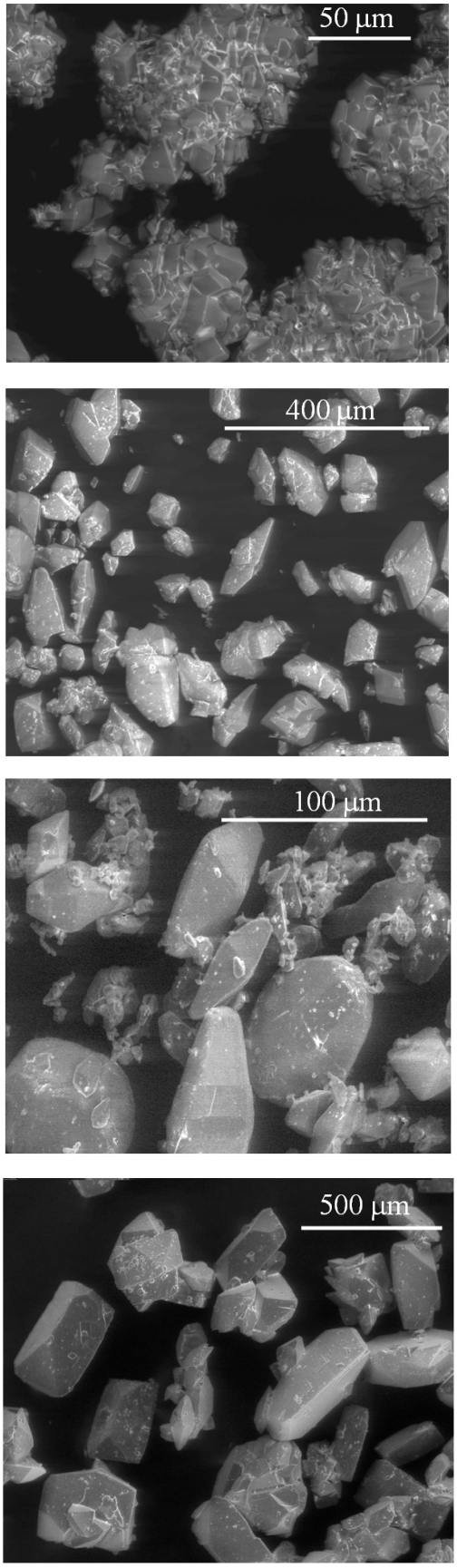

Figure 1. SEM images of (a) raw CL-20, prepared ε-CL-20 using, (b) solvent evaporation without in-situ ultrasonication, (c) solvent evaporation with in-situ ultrasonication, and (d) precipitation methods.

shown in Figs.1(b), 1(c), and 1(d) as compared with those of raw CL-20. The crystal morphology of prepared ε-CL-20 by solvent evaporation without ultrasonication method show dominantly bi-pyramidal shape as shown in Fig.1(b) with sharp edges. However, as shown in Fig.1(c), the sharp edge of bi-pyramidal crystal is smoothened increasingly using in-situ ultrasonication. Further, in-situ ultrasonication batch also show few bigger size near spherical particles surrounded by fine size particles. It clearly attributes that in-situ ultasonication greatly helps to promote sharp edge free crystals during crystallisation. The crystal morphology of prepared ε-CL-20 by precipitation method show dominantly lozenge shape as shown in Fig. 1(d). The observed crystal habits are well matched with ε-CL-20 crystal morphology as reported in the literature[9]. By conducting several batches, the reproducible mean particle size of prepared ε-CL-20 by solvent evaporation method with, without in-situ ultrasonication and precipitation methods is in the range of about 30 µm - 40 µm, 150 µm - 200 µm and 150 µm - 300 µm, respectively as shown in Table 1. The typical particle size distribution of prepared ε-CL-20 using both solvent evaporation methods and precipitation methods along with raw CL-20 is shown in *Appendix* in the supporting information.

Table 1. Recovery, purity and mean particle size of ε-CL-20 using solvent evaporation and precipitation methods

Sample	Recovery (%)	Chemical purity (%)[a]	Polymorphic purity (% ε)[b]	Mean particle size range (µm)[c]
ε-CL20[d]	85-90	98	> 95	150-200
ε-CL20[e]	85	98	> 95	30-40
ε-CL20[f]	85-90	98	> 95	150-300

Note: [a] Determined by HPLC, [b]Determined by FTIR and Raman (see details from the text), [c]Determined by Malvern particle size analyser, [d]Prepared by solvent evaporation method, [e]Prepared by solvent evaporation method with insitu ultrasonication method, and [f] Prepared by precipitation method.

To begin with characterisation of prepared ε-CL-20 by solvent evaporation and precipitation methods, we analyzed starting material raw CL-20. X-ray powder diffraction pattern for raw CL-20 and prepared ε-CL-20 is shown in Fig. 2 along with α-CL-20 and ε-CL-20 library standard over the region of 10-45° [12,13]. It can be seen from Figs 2 (a) and 2 (b) that X-ray powder diffraction profile of raw CL-20 is well comparable with the library standard of α-CL-20. The prominent features of raw CL-20 at 2θ = 12.0°, 13.6°, 13.8°, 17.4°, 17.9°, 20.1°, 24.9°, 27.4°, 27.9°, and 28.7° are essentially those of α-CL-20. Figure 3 shows the infrared spectra of raw CL-20 and prepared ε-CL-20 over the region 400 cm^{-1} – 4000 cm^{-1}. While authors have recorded the spectra over the region 400 cm^{-1} – 4000 cm^{-1}, only the regions 1700 cm^{-1} – 1500 cm^{-1} and 900 cm^{-1} – 600 cm^{-1} are shown, as these are the regions that carry information on the polymorphs of CL-20. Table 2 shows the infrared frequencies of raw CL-20 and prepared ε-CL-20 along with the literature

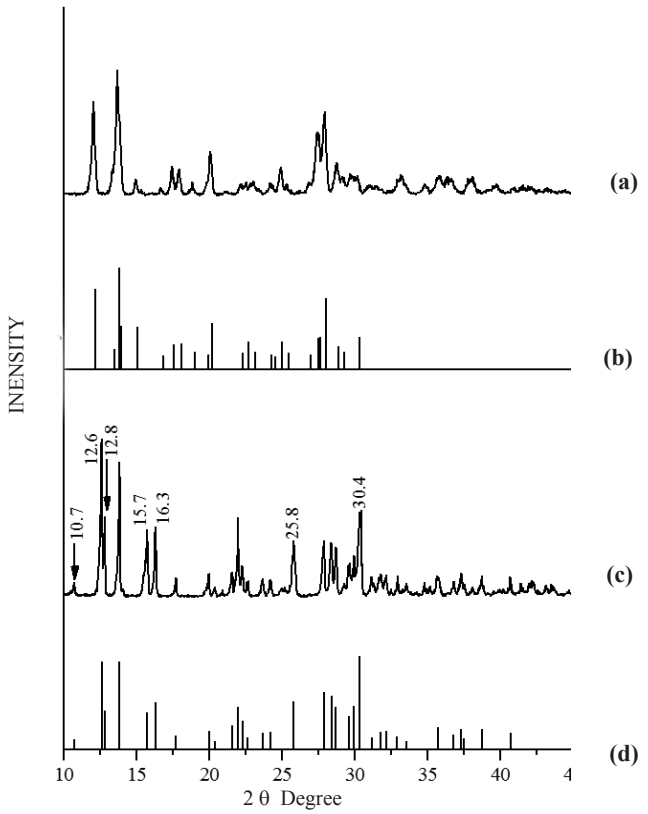

Figure 2. X-ray powder diffraction patterns of CL-20 polymorphs. Trace 2(a) and 2(c) are the experimental spectrum of raw CL-20 and ε-CL-20, respectively. Trace 2(b) and 2(d) are library standards of α-CL-20 and ε-CL-20 from[12, 13], respectively.

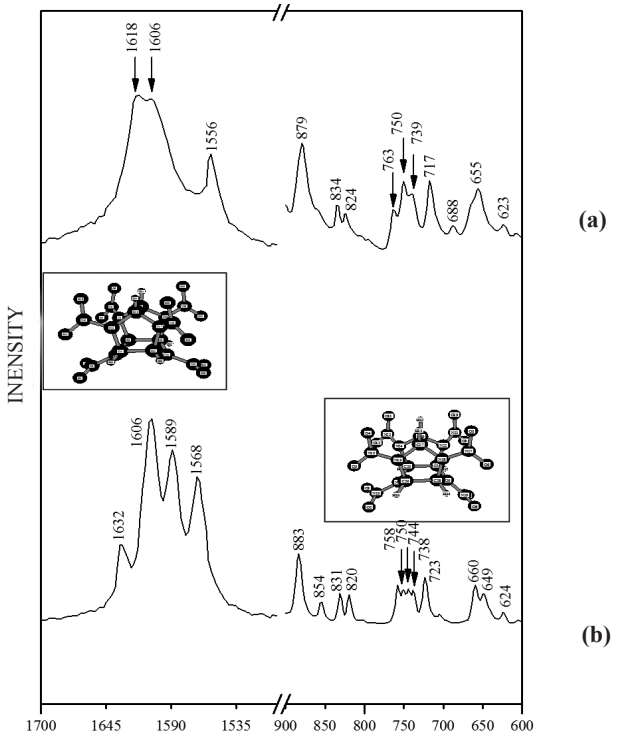

Figure 3. Experimental FTIR spectra of (a) raw CL-20 and (b) prepared ε-CL-20 in the regions of 1700 cm^{-1} - 1500 cm^{-1} and 900 cm^{-1} - 600 cm^{-1}. Insert figures show the molecular structure of CL-20 polymorphs.

Table 2. The experimental infrared frequencies of raw CL-20 and prepared ε-CL-20 along with the literature data[16]

Experiment (cm^{-1})		Literature (cm^{-1})				Tentative mode assignment
Raw CL-20	**ε-CL-20**	**α-CL-20**	**ε-CL-20**	**β-CL-20**	**γ-CL-20**	
445 w	445 vw					NNO bend
471 w	465 vw					NNO bend
513 w	525 vw					NNO bend
562 w	567 w					NNO bend
588 w	590 w					Ring def
607 w	605 vw					Ring def
623	624 vw					Ring def
655 m, 688 m	660 w, 649 w					NO bend
	687 w					NO bend
	705 vw		705.1			NO bend
717 m	723 w	718	723.9	718.9	719.5	NO bend; NNO_2 bend
739 w, 750 w, 763 w	738 w, 744 w, 750 w, 758 w	746.5,751.1, 764.9	738.2, 744.5, 751.4, 758.2	746.4, 766.8	741, 755.8, 764.1	ONO bend; NO bend
824 w, 834 w	820 w, 831 w	825.3, 835.4	820.2, 831.6	835.4	831.7, 834.4	ONO bend; NO bend
859 w	854 w	860.2	855.4		858.3	ONO bend; NO bend
879 s	883 m	881.7	883.8	882.9	879.2	ONO bend; NO bend
					892	ONO bend; NO bend
903 w	912 w	904.3	913.2	907.7	909.4	Ring str; NN str
951 s	937 m, 943 m	951.7	938.3, 944.4	944.9, 959.2	938.1, 958.8	Ring str; NN str
989 w	980 w	989.2, 990.7	980.9	991.8	970.6	Ring str; NN str
	1020 w		1022.1			Ring str; NN str
1052 m	1050 m	1052.4	1051.6	1052.3	1043.8	Ring str; NN str
1078 w		1078.3				Ring str; NN str
1094 w	1087 w	1094.9	1087.2			Ring str; NN str
1122 w	1124 w, 1136 w	1121.1	1125.1, 1139.2	1094.7	1080.4, 1106.1	Ring str
1165 w	1182 w, 1191 w	1168.1	1182.5, 1191.7	1154.4, 1171.8, 1178.6	1153, 1180.4	CH bend ; NO str sym
1228 m	1218 w					CH bend ; NO str sym
1266 vs, 1291 vs	1265 vs					CH bend ; NO str sym
	1285 vs, 1298 vs					CH bend ; NO str sym
1330 vs	1329 vs, 1338 vs, 1348 vs					CH bend ; NO str sym
1380 w	1382 vw					CH bend ; NO str sym
1556 s	1568 vs					NO str sym
	1589 vs					NO str sym
1606 vs, 1618 vs	1606 vs					NO str asym
	1632 m					NO str asym
3024 m	3017 m					CH str
3037 m	3036 m					CH str
3052 m	3045 m					CH str
3605 vw						OH str
3694 vw						OH str

Note: vs - very strong; s - strong; m - medium; w - weak; vw - very weak.

value. The regions of 1700 cm^{-1} - 1500 cm^{-1} and 900 cm^{-1} – 600 cm^{-1} correspond to the NO_2 stretching and mostly bending and deformation (NNO bending, ring deformation, *NO* out of plane bending and ONO bending) vibrations, respectively. The main infrared spectral features of raw CL-20 occuring at 623 cm^{-1}, 655 cm^{-1}, 688 cm^{-1}, 717 cm^{-1}, 739 cm^{-1}, 750 cm^{-1}, 763 cm^{-1}, 824 cm^{-1}, 834 cm^{-1}, 879 cm^{-1}, 1556 cm^{-1}, 1606 cm^{-1}, and 1618 cm^{-1} as shown in Fig. 3(a), which is well comparable with α-CL-20 as reported in the literature[14,16]. We then recorded raw CL-20 and prepared ε-CL-20 spectrum using dispersed Raman spectrometer in the region of 100 cm^{-1} - 4000 cm^{-1} as shown in Fig. 4. Table 3 shows the Raman frequencies of raw CL-20 and prepared ε-CL-20 along with the literature value. The main Raman spectral features of raw CL-20 occur at 268 cm^{-1}, 280 cm^{-1}, 793 cm^{-1}, 822 cm^{-1}, 839 cm^{-1}, and 858 cm^{-1} over the regions of 260 cm^{-1} – 300 cm^{-1} and 740 cm^{-1}– 880 cm^{-1} as shown in Fig. 4(a). As observed in X-ray powder diffraction and infrared experimental results, Raman spectrum of raw CL-20 is also well comparable with literature reported α-CL-20 forms[16,17]. It confirms that the starting material raw CL-20 corresponds to α-CL-20 polymorphic phase. X-ray powder diffraction profile of prepared ε-CL-20 showed the characteristic peaks at about 2θ = 10.7°, 12.6°, 12.8 °, 15.7°, 16.3°, 25.8°, and 30.4° as compared those of raw CL-20 as shown in Fig. 2(b). As can be seen from Figs. 2 (c) - 2(d), X-ray powder diffraction features of prepared ε-CL-20 matched well with previously reported ε-CL-20 form[12,13]. The main infrared features of prepared ε-CL-20 are shown in Fig. 3(b). The presence of quartet and equivalent doublet near 750 cm^{-1} (738 cm^{-1}, 744 cm^{-1}, 750 cm^{-1} and 758

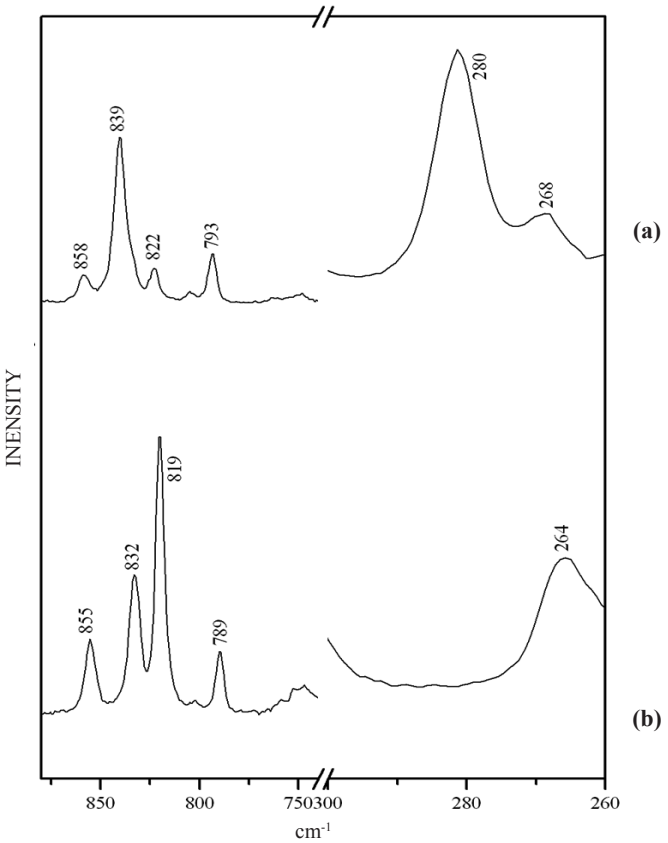

Figure 4. Experimental Raman spectra of (a) raw CL-20 and (b) prepared ε-CL-20 in the regions of 260 cm^{-1} - 300 cm^{-1} and 740 cm^{-1} - 880 cm^{-1}.

Table 3. The experimental Raman frequencies of raw CL-20 and prepared ε-CL-20 along with the literature (ref. 16) data

Experiment (cm^{-1})		Literature (cm^{-1})			
Raw CL-20	**ε-CL-20**	**α-CL-20**	**ε-CL-20**	**β-CL-20**	**γ-CL-20**
115, 130 vs	127, 136 s				
164 w	158 w				
	193 m				
	219 w				
226 m					
257 w					
268 m	264 w		267		270
280 vs		283		284	287
310 w, 318 w	318 s				
336 m	344 w				
365 w, 374 w	369, 383 w				
401 w	409 vw				
450 w, 471 w	446, 465 vw				
515 w	527 m				
564 vw	568 vw				
597 vw	580 vw				
608 vw	591 vw				

Experiment (cm^{-1})		Literature (cm^{-1})			
Raw CL-20	**ε-CL-20**	**α-CL-20**	**ε-CL-20**	**β-CL-20**	**γ-CL-20**
625 vw	624 vw				
656 vw	643 vw				
666 vw	660 vw				
689 vw					
717 vw	721 vw				
749 vw, 763 vw	747, 752 vw	762	755	763	762
793 m	789 m	795	791	792	795
822 m	819 s	825	820	805	836
839 vs	832 m	842	832	835	849
858 m	855 m	861	857	854	861
906 w	912 vw				
958 w	940 m				
989 m	983 m	1000		1000	1020
1048 w	1051 w	1054	1055	1055	1060
1093 w	1088 w	1095	1085	1076, 1090	1083
	1124 w		1125	1125	1105, 1120
1148vw, 1164 vw		1150, 1170, 1192		1130, 1155, 1175	1148
	1183 vw		1180	1188	1180
	1204, 1219 vw				
1230 w	1249 m				
1264 s	1262 m				
	1276 m				
1300 s	1310 vs				
1328, 1333 vs	1336 s				
1382, 1388 w	1383 m				
1500 w	1503 vw				
1557 w	1561 w				
1582, 1603 w	1578, 1597 w				
	1608, 1616 w				
1630 m	1625 m				
3027 s	3019 w	3028	3020	3035	3035
3038 m	3032 s	3036	3031	3045	3044
3056 vs	3048 vs	3058	3048	3055	3062

Note: vs - very strong; s - strong; m - medium; w - weak; vw - very weak.

cm^{-1}) and 825 cm^{-1} (820 $cm^{-1}$and 831 cm^{-1}) cm^{-1}, respectively in Fig. 3(b) establish the purity of ε-CL-20. Further, ε-CL-20 shows a quartet-like near 1600 cm^{-1} (1568 cm^{-1}, 1589 cm^{-1}, 1606 cm^{-1} and 1632 cm^{-1}) in the region of asymmetric NO_2 stretching vibration. ε-CL-20 shows a distinct single Raman feature at 264 cm^{-1} over the region of 260 cm^{-1} - 300 cm^{-1}, corresponds to ring deformation, where it is at 280 cm^{-1} for α-CL-20 along with weak feature at 268 cm^{-1} as shown in Fig. 4(b). We also note that the β-CL-20 and γ-CL-20 polymorphs also occur at 284 cm^{-1}, 287 cm^{-1}, and 270 cm^{-1}, respectively in the region of 260-300 cm^{-1} as reported in the literature[16,17]. Hence, the absence of feature near at 280 cm^{-1} in prepared ε-CL-20 clearly indicates the higher polymorphic purity of ε-CL-20, which was assigned to be > 95%. The polymorphic purity of different batches of ε-CL-20 by solvent evaporation and precipitation methods show > 95%. Other Raman spectral features of prepared ε-CL-

20 in the region of 740 cm^{-1}- 880 cm^{-1}occur at 789 cm^{-1}, 819 cm^{-1}, 832 cm^{-1}, and 855 cm^{-1} as shown in Fig. 4(b). The thermal behavior of raw CL-20 and prepared ε-CL-20 are recorded in nitrogen atmosphere when heated in crimped Aluminum pan from 30 ºC to 300 ºC at a heating rate of 10 °C/min. Sample sizes of about 0.2 mg were employed to study decomposition behavior. However, to see solid-solid phase transition peak unambiguously, sample size increased of about 2 mg. The DSC curve in Fig. 5(a) demonstrates an endothermic behaviour of raw CL-20 with a peak temperature, T_p= 174 ± 1 ºC. This peak is assigned to solid-solid α → γ phase transition and the peak temperature of solid-solid ε → γ phase transition is observed at 160 ± 1 ºC Fig. 5(b), which are well comparable with value in reported literature[18]. Later than the solid-solid phase transition, the DSC profile exhibits a single step exothermic thermal decomposition for both raw CL-20 and ε-CL-20. Figure 6(a) shows the onset and peak temperature of single step exothermic thermal decomposition behaviour of raw CL-20 at T_o= 235 ± 1 ºC and T_p= 253 ± 1 ºC, respectively. Similarly, the onset and peak temperature of exothermic thermal decomposition behavior of prepared ε-CL-20 is recorded at T_o= 234 ± 1 ºC and T_p= 252 ± 1 ºC, respectively as shown in Fig. 6(b).

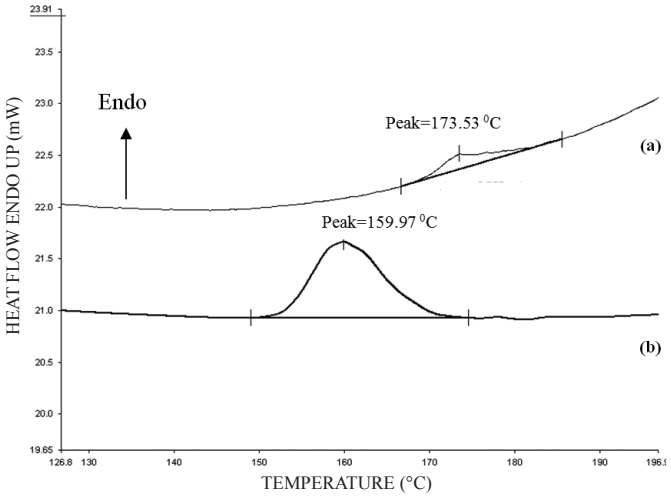

Figure 5. Endothermic phase transition (DSC, 10 °C/min, N_2 atmosphere, 2 mg) of (a) raw CL-20 and (b) prepared ε-CL-20 in the temperature range of 127-196 °C.

Table 4 shows true density characteristics of raw CL-20 and prepared ε-CL-20 by precipitation method along with the reported values. The measured true density using Helium gas pycnometer of raw CL-20 with the total moisture content of about 1.1% (weight percent) was 1.987 g/cm^3, which is close to the ideal crystal density value of α-CL-20 hydrate (2.001 g/cm^3 - 1.981 g/cm^3) as reported in the literature[4]. However, the true density of prepared ε-CL-20 with 100 g batch and 500 g batch size by precipitation method were determined to be 2.038 g/cm^3 and 2.043 g/cm^3, respectively, which is well consistent with the maximum true density of ε-CL-20 crystal suggested by Johnston and Wardle[15]. The reported ideal crystal density of ε-CL-20 is 2.044 g/cm^3. The void percentage of prepared ε-CL-20 with 100 g batch and 500 g batch size was quantitatively estimated from density difference in compared

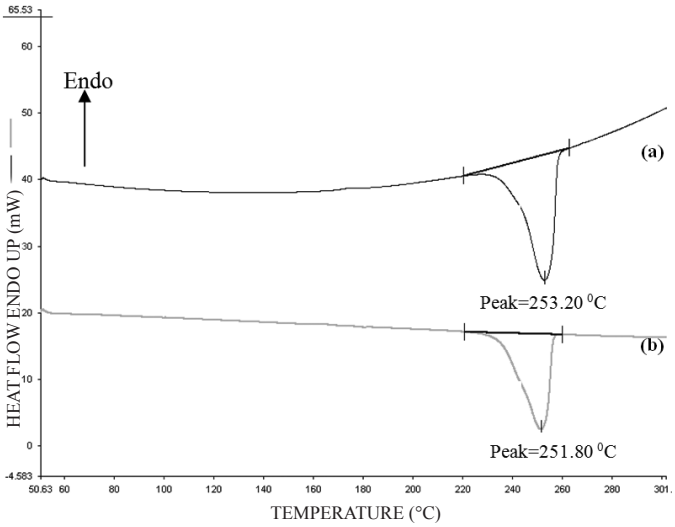

Figure 6. DSC measurement (10 °C/min, 0.2 mg) in the presence of nitrogen atmosphere of (a) raw CL-20 and (b) prepared ε-CL-20 in the temperature range of 50 °C - 300 °C.

to ideal crystal density and was calculated to be 0.29% and 0.05%, respectively. The low void percentage of prepared ε-CL-20 signifies the good crystal quality as reported in the literature[11]. It is well known that shock sensitivity is reduced with the density growth of material, which suggests our prepared ε-CL-20 may have reduced shock sensitive[19] than those of raw CL-20, which will be subject of our future studies. Further, the total moisture percentage of prepared ε-CL-20 is about ≤ 0.1%, which is an essential criteria for formulation of high explosives and propellant compositions.

Table 4. Density characteristics of raw CL-20 and prepared ε-CL-20 by precipitation method along with the reported values

Sample	True density[a] (g/cm^3)	Void[b] (%)	TMD[c] (%)
Raw CL-20[d]	1.987	-	-
ε-CL20 (100 g batch)	2.038	0.29	99.71
ε-CL20 (500 g batch)	2.043	0.05	99.95
ε-CL20-reported[e]	2.019-2.043	1.22-0.05	98.78 - 99.95

Note : [a] Measured using He gas pycnometer. The error in the measured true density value is typically ± 0.0002 g/cm^3. [b] Void (%) = [(2.044 – True density)/2.044]*100. [c] TMD (%) = 100 - Void (%). [d] Total moisture content of 1.1% (weight percentage) using Karl Fischer method. [e] Taken from ref. 11.

4. CONCLUSION

Preparation of the ε-CL-20 polymorph is carried out from raw CL-20 by solvent evaporation with and without in-situ ultrasonication and precipitation methods. Preparation of ε-CL-20 by precipitation method is scaled upto batch size of 500 g. Prepared ε-CL-20 were well characterised using HPLC, vibrational spectroscopic, X-ray powder diffraction, scanning electron microscopic and DSC techniques. Raw CL-20 was assigned to be α-CL-20. The chemical and polymorphic

purity of prepared ε-CL-20 was found to be about 98% and > 95%, respectively and their obtained crystal morphology is dominantly bi-pyramidal or lozenge crystal shapes. Using solvent evaporation coupled with in-situ ultrasonication method, the sharp edge of bipyramidal crystal is increasingly smoothened and also shows few bigger size spherical particles surrounded by fine size particles. The mean particle size of prepared ε-CL-20 by solvent evaporation coupled with in-situ ultrasonication method is about 30 µm – 40 µm. The measured true density of prepared ε-CL-20 by precipitation method with 100 g and 500 g batch scale using He gas pycnometer was 2.038 g/cm^3 and 2.043 g/cm^3, respectively. The prepared ε-CL-20 has high true density with less percentage of voids, less total moisture content and free from agglomeration as compared with the starting raw CL-20.

ACKNOWLEDGEMENTS

The authors express gratitude to Director, High Energy Materials Research Laboratory (HEMRL), Pune for publication of the article. Authors are also thankful to Mr S.K. Sahoo and Mr P. Paramasivan from HEMRL, for their help in powder XRD and density characterisations, respectively.

REFERENCES

1. Nielsen, A.T. Polycyclic amine chemistry. *In* Chemistry of energetic materials, edited by G.A. Olah & D.R. Squire. Academic Press, San Diego, US, 1991, pp. 95-124
2. Simpson, R.L.; Urtiew, P.A.; Ornellas, D.L.; Moody, G.L.; Scribner, K.J. & Hoffman, D.M. CL-20 performance exceeds that of HMX and its sensitivity is moderate. *Propellants, Explos., Pyrotech.*, 1997, **22**(5), 249-55.
3. Li, J. & Brill, T.M. Kinetics of solid polymorphic phase transition of CL-20. *Propellants, Explos., Pyrotech.*, 2007, **32**(4), 326-330.
4. Nielsen, A.T.; Chafin, A.P.; Christian, S.L.; Moore, D.W.; Nadler, M.P.; Nissan, R.A. & Vanderah, D.J. Synthesis of polyazapolycyclic caged polynitramines. *Tetrahedron,* 1998, **54**(39), 11793-11812.
5. Foltz, M.F.; Coon, C.L.; Garcia, F. & Nicholas III, A.L. Thermal stability of the polymorphs of hexanitrohexaazaisowurtzitane, Pt I. *Propellants, Explos., Pyrotech.*, 1994, **19**(1), 19-25.
6. Johnson, N.C. CL-20 sensitivity round robin. Indian Head Division Naval Surface Warfare Center, User Report No. MD 20640-5035, September 2003.
7. Hamilton, R.S.; Mancini, V.; Nelson, C. & Dressen, S.Y. High temperature crystallisation of 2,4,6,8,10,12-hexanitro-2,4,6,8,10,12-hexaazatetracyclo [5.5.0. 05,903,11]—dodecane. US Patent No. 7288648, 30 October, 2007.
8. Johnston, H.E. & Wardle, R.B. Process of crystallising 2,4,6,8,10,12-hexanitro-2,4,6,8,10,12,-hexaazatetracyclo [5.5.0.0.5,903,11]-dodecane. US Patent No. 5874574, 23 February, 1999.
9. Mersmann, A. Crystallisation technology handbook. Ed. 2. Marcel Dekker, New York, 2001.
10. Hoffman, D.M. Void density distribution in 2,4,6,8,10,12-Hexanitro-2,4,6,8,10,12-hexaazaisowurtzitane (CL-20) prepared under various conditions. *Propellants, Explos., Pyrotech.*, 2003, **28**(4), 194-200.
11. Caulder, S.M.; Buess, M.L. & Nock, L.A. An analytical study of the crystal quality of e-hexanitrohexaazaisowurtzitane (CL-20) synthesized using several different crystallisation techniques and intermediate precursors. *Sci. Tech. Energetic Materials*, 2005, **66**, 406-409.
12. Engel, W. ICDD Grant-in-Aid. Fraunhofer-Inst. of Chemische Technologie, Pfinztal-Berghausen, Germany, 1999.
13. Engel, W. ICDD Grant-in-Aid. Fraunhofer-Inst. of Chemische Technologie, Pfinztal-Berghausen, Germany, 2000.
14. Holtz, E.V.; Ornellas, D.; Foltz, M.F. & Clarkson, J.E. The solubility of e-CL-20 in selected materials. *Propellants, Explos., Pyrotech.*, 1994, **19**(4), 206-212.
15. Wardle, R.B.; Johnston, G.; Hinshaw, J.C.; Braithwaite, P. Synthesis of the cased nitramine HNIW (CL-20). Paper presentated at 27th International Annual Conference of ICT, 1996.
16. Kholod,Y.; Okovytyy, S.; Kuramshina, G. & Qasim, M. An analysis of stable forms of CL-20: A DFT study of conformational transitions, infrared and Raman spectra. *J. Molecular Structure*, 2007, **843**(1-3), 14-25.
17. Gorb, L.; Leszczynski, J.; Goede, P.; Latypov, N. & Ostmark, H. Fourier transform Raman spectroscopy of the four crystallographic phases of α, β, γ and ε 2,4,6,8,10,12-Hexanitro-2,4,6,8,10,12-hexaazatetracyclo[5.5.0.0^{5,9}.0^{3,11}] dodecane (HNIW, CL-20). *Propellants, Explos., Pyrotech.,* 2004, **29**(4), 205-08.
18. Foltz, M.F.; Coon, C.L.; Garcia, F. & Nicholas III, A.L. Thermal stability of the polymorphs of hexanitrohexaazaisowurtzitane, Pt II. *Propellants, Explos., Pyrotech.*, 1994, **19**(3), 133-44.
19. Antoine, E.D.M.; Heijden, Van der & Bouma, R.H.B. Crystallisation and characterisation of RDX, HMX and CL-20. *Crystal Growth Design*, 2004, **4**(5), 999-1007.

Contributors

Shri Mrinal Ghosh obtained his MTech from Indian Institute of Technology, Delhi in 2005. Presently working as Scientist C at High Energy Materials Research Laboratory (HEMRL), Pune. His research area includes: Polymorphism in crystalline explosive materials their preparation, characterisation using vibrational spectroscopy and electron microscopic techniques.

Dr V. Venkatesan obtained PhD (Chemistry) from Indira Gandhi Centre for Atomic Research, Kalpakkam in 2003. Presently, he is working as Scientist 'D' at HEMRL, Pune. His research and work experiences include: condensed phase and gas phase spectroscopy, crystallisation, polymorphism, molecular and its cluster structure determination and computational calculations.

Dr AK Sikder presently working as an Associate Director at the HEMRL, Pune. He has published about 85 research papers in national/ international journals. Earlier he worked on highly toxic organophosphorus compounds used as chemical warfare agents and their antidotes. His research work includes: High energy materials in a wide spectrum of subjects of defence interest.

Dr (Mrs) Nirmala Sikder obtained her PhD from Jiwaji University, Gwalior, in 1996. Presently she is working as a Scientist at the HEMRL, Pune. She has published more than 35 papers in national/international journals. Earlier she worked on synthesis, characterisation and hydrolysis studies on toxic organophosphorus compounds. Her research includes: Synthesis of high energy materials and their instrumental analysis.

Appendix

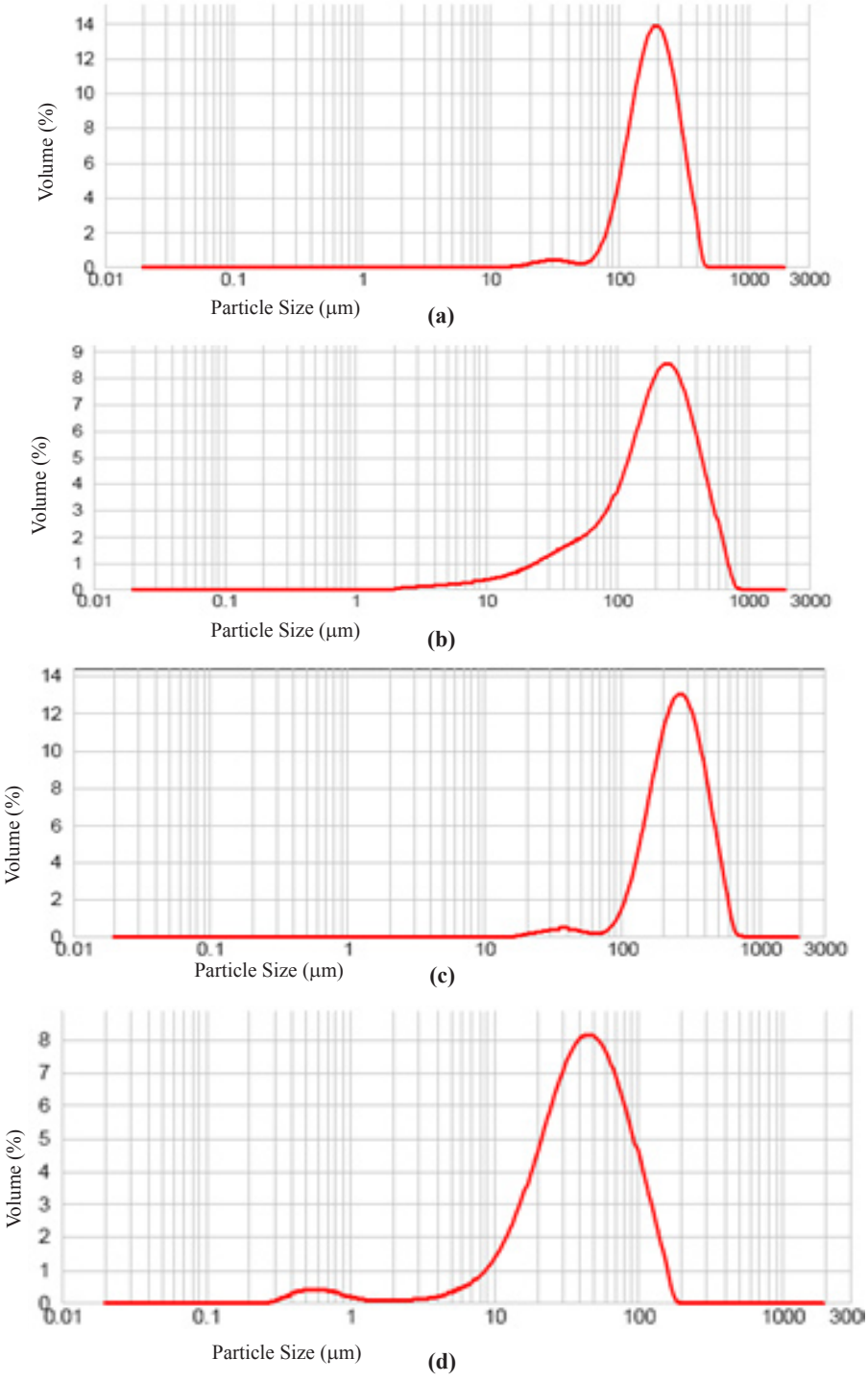

Figure 1S. Particle size distribution of (a) raw CL-20, prepared ε-CL-20 using (b) solvent evaporation without in-situ ultrasonication, (c) solvent evaporation with in-situ ultrasonication, and (d) precipitation methods.